Available online at www.sciencedirect.com
ScienceDirect
Signal Processing 87 (2007) 68–78
SIGNAL PROCESSING
www.elsevier.com/locate/sigpro

Adaptive beamforming for binary phase shift keying communication systems

S. Chen*, S. Tan, L. Hanzo

School of Electronics and Computer Science, University of Southampton, Southampton SO17 1BJ, UK

Received 27 September 2005; received in revised form 21 February 2006; accepted 11 April 2006
Available online 8 June 2006

Abstract

The paper revisits adaptive beamforming assisted receiver for multiple antenna aided multiuser systems that employ binary phase shift keying (BPSK) modulation. The standard minimum mean square error (MMSE) design is based on the criterion of minimising the mean square error (MSE) between the beamformer's desired output and complex-valued beamformer's output. Since the desired output for BPSK systems is real-valued, minimising the MSE between the beamformer's desired output and real-part of the beamformer's output can significantly improve the bit error rate (BER) performance, and we refer to this alternative MMSE design as the real-valued MMSE (RV-MMSE) to contrast to the standard complex-valued MMSE (CV-MMSE) design. The minimum BER (MBER) design however still outperforms the RV-MMSE solution, particularly for overloaded systems where degree of freedom of the antenna array is smaller than the number of BPSK users. Adaptive implementation of this RV-MMSE beamforming design is realised using a least mean square (LMS) type adaptive algorithm, which we refer to as the RV-LMS, in comparison to the standard CV-LMS algorithm. The RV-LMS adaptive beamformer is shown to have a similar computational complexity as the adaptive MBER beamforming implementation known as the least bit error rate (LBER), imposing only half of the computational requirements of the CV-LMS algorithm.

Keywords: Adaptive beamforming; Binary phase shift keying modulation; Minimum mean square error; Minimum bit error rate

1. Introduction

The ever-increasing demand for mobile communication capacity has motivated the development of adaptive antenna array-assisted spatial processing techniques [1–12] in order to further improve the achievable spectral efficiency. A technique that has shown real promise in achieving substantial capacity enhancements is the use of adaptive beamforming with antenna arrays. Through appropriately combining the signals received by the different elements of an antenna array, adaptive beamforming is capable of separating signals transmitted on the same carrier frequency, and thus provides a practical means of supporting multiusers in a space division multiple access scenario. Classically, the beamforming process is carried out by minimising

*Corresponding author. Tel.: +44 23 8059 6660; fax: +44 23 8059 4508.
E-mail addresses: sqc@ecs.soton.ac.uk (S. Chen), st104r@ecs.soton.ac.uk (S. Tan), lh@ecs.soton.ac.uk (L. Hanzo).

0165-1684/$ - see front matter © 2006 Elsevier B.V. All rights reserved.
doi:10.1016/j.sigpro.2006.04.007

the mean square error (MSE) between the desired output and the beamformer's output. For a communication system, however, it is the bit error rate (BER) that really matters. Adaptive beamforming based on directly minimising the system's BER has been proposed for binary phase shift keying (BPSK) and quadrature phase shift keying modulation schemes [13–15].

This paper re-visits adaptive beamforming for BPSK systems. Such an adaptive beamforming-assisted receiver is characterised by an adaptive spatial filter with complex-valued (CV) input signal and real-valued (RV) desired output. The standard minimum MSE (MMSE) design [16–18] seeks the CV beamformer's weight vector that minimises the MSE between the beamformer's desired output and the CV beamformer's output. We will refer to this MMSE solution as the CV-MMSE. Since the beamformer's desired output, namely the desired user's transmitted symbol, is RV, minimising the MSE between the beamformer's desired output and the real part of the beamformer's output can significantly improve the achievable system's BER performance. We will refer to this alternative MMSE design as the RV-MMSE, to contrast to the standard CV-MMSE design. Since the RV-MSE criterion is quadratic, the RV-MMSE design admits a closed-form solution just as the case of the CV-MMSE solution. In this aspect, the RV-MMSE solution is better than the minimum BER (MBER) design [13], which requires a numerical solution. The MBER beamforming design however is the true optimal solution and it generally outperforms the RV-MMSE solution.

It is generally believed that the CV-MMSE beamforming-assisted receiver has the capacity of supporting up to the same number of users as the number of antenna elements, and a practical rule is that the number of antennas should not be smaller than the number of users supported. This is to ensure that the system has a sufficient degree of freedom to cancel the interfering signals. However, using the RV-MMSE design, the system should be capable of supporting users up to twice the number of antenna elements. A heuristic explanation is as follows. The design criterion of the RV-MMSE beamforming is RV or one dimensional, while the signal of each antenna array element is CV or two dimensional. Thus, degree of freedom of the antenna array is twice the number of antenna array elements. Hence, for the CV-MMSE beamforming-assisted receiver, the system is overloaded if the number of users is more than the number of antenna elements. But for the RV-MMSE beamforming-assisted receiver, the system is overloaded if the number of users is more than twice the number of antenna elements. The MBER design, on the other hand, is capable of providing a system capacity beyond the limit of the RV-MMSE solution. These points will be illustrated by a simulation example.

Adaptive implementations are compared for the three beamforming designs. The CV-MMSE solution can adaptively be realised using the least mean square (LMS) algorithm [16–18], and we will refer to this standard LMS algorithm as the CV-LMS. The adaptive implementation of the RV-MMSE design based on a stochastic gradient adaptive algorithm also lead to a LMS-type algorithm, which we refer to as the RV-LMS algorithm. Since this RV-LMS algorithm is a "special" case of the LMS algorithm, standard convergence analysis (e.g. [18]) for the general LMS algorithm also applies to this RV-LMS algorithm. An adaptive implementation of the MBER solution is known as the least bit error rate (LBER) algorithm [13]. Because the BER criterion is highly complicated and certainly non-quadratic, convergence analysis of the LBER algorithm is a difficult task. Basically, initial condition can significantly influence convergence rate as well as the steady-state BER. Nevertheless, convergence analysis for the general stochastic gradient-based adaptive algorithm investigated in [19] can be applied to the LBER algorithm, since the LBER algorithm belongs to the class of general stochastic gradient-based adaptive algorithms. In terms of computational complexity, the RV-LMS algorithm is similar to the LBER algorithm, imposing only half of the computational requirements of the CV-LMS algorithm.

2. System model

The system consists of M users, and each user transmits a BPSK signal on the same carrier frequency $\omega = 2\pi f$. The receiver is equipped with a linear antenna array consisting of L uniformly spaced elements. Assume that the channel is narrow-band which does not induce intersymbol interference. Then the symbol-rate received signal samples at the antenna array's output can be

expressed as

$$x_l(k) = \sum_{i=1}^{M} A_i b_i(k) e^{j\omega t_l(\theta_i)} + n_l(k) = \bar{x}_l(k) + n_l(k), \quad 1 \leqslant l \leqslant L, \tag{1}$$

where $t_l(\theta_i)$ is the relative time delay at antenna element l for source i with θ_i being the direction of arrival for source i, $n_l(k)$ is a CV Gaussian white noise process with $E[|n_l(k)|^2] = 2\sigma_n^2$, A_i is the CV channel coefficient for user i, and $b_i(k)$ is the kth symbol of user i which takes the value from the BPSK symbol set $\{\pm 1\}$. Without the loss of generality, source 1 is the desired user and the rest of the sources are interfering users. The desired-user signal-to-noise ratio is defined by $\mathrm{SNR} = |A_1|^2\sigma_b^2/2\sigma_n^2$ and the desired signal to interferer i ratio is given by $\mathrm{SIR}_i = A_1^2/A_i^2$, for $2 \leqslant i \leqslant M$, where $\sigma_b^2 = 1$ is the symbol energy. The received signal vector $\mathbf{x}(k) = [x_1(k)\ x_2(k)\ \ldots\ x_L(k)]^{\mathrm{T}}$ can be expressed as

$$\mathbf{x}(k) = \mathbf{P}\mathbf{b}(k) + \mathbf{n}(k) = \bar{\mathbf{x}}(k) + \mathbf{n}(k), \tag{2}$$

where $\mathbf{n}(k) = [n_1(k)\ n_2(k)\ \ldots\ n_L(k)]^{\mathrm{T}}$, the system matrix

$$\mathbf{P} = [\mathbf{p}_1\ \mathbf{p}_2\ \ldots\ \mathbf{p}_M] = [A_1\mathbf{s}_1\ A_2\mathbf{s}_2\ \ldots\ A_M\mathbf{s}_M] \tag{3}$$

with the steering vector for source i

$$\mathbf{s}_i = [e^{j\omega t_1(\theta_i)}\ e^{j\omega t_2(\theta_i)}\ \ldots\ e^{j\omega t_L(\theta_i)}]^{\mathrm{T}}, \tag{4}$$

and the transmitted user symbol vector $\mathbf{b}(k) = [b_1(k)b_2(k)\ \ldots\ b_M(k)]^{\mathrm{T}}$.

We consider the detection of the desired user's transmitted symbols using a linear beamformer, whose soft output is given by

$$y(k) = \mathbf{w}^H\mathbf{x}(k) = \mathbf{w}^H(\bar{\mathbf{x}}(k) + \mathbf{n}(k)) = \bar{y}(k) + e(k), \tag{5}$$

where $\mathbf{w} = [w_1\ w_2\ \ldots\ w_L]^{\mathrm{T}}$ is the CV beamformer weight vector and $e(k)$ is Gaussian distributed with zero mean and $E[|e(k)|^2] = 2\sigma_n^2\mathbf{w}^H\mathbf{w}$. The beamformer's hard decision is given by

$$\hat{b}_1(k) = \mathrm{sgn}(y_R(k)), \tag{6}$$

where $\hat{b}_1(k)$ denotes the estimate of $b_1(k)$ and $y_R(k) = \Re[y(k)]$ denotes the real part of $y(k)$.

3. Beamformer designs

The task of designing the beamformer (5) is to choose the beamformer's weight vector $\mathbf{w}$ according to some design criterion.

3.1. Complex-valued minimum mean square error design

Classically, the beamformer's weight vector $\mathbf{w}$ is determined by minimising the MSE metric of

$$J_{\mathrm{MSE}}(\mathbf{w}) = E[|b_1(k) - y(k)|^2]. \tag{7}$$

The gradient of $J_{\mathrm{MSE}}(\mathbf{w})$ with respect to $\mathbf{w}$ is given by

$$\nabla J_{\mathrm{MSE}}(\mathbf{w}) = E[-(b_1(k) - y(k))^*\mathbf{x}(k)] = -\mathbf{p}_1 + (\mathbf{P}\mathbf{P}^H + 2\sigma_n^2\mathbf{I}_L)\mathbf{w}. \tag{8}$$

Setting the gradient $\nabla J_{\mathrm{MSE}}(\mathbf{w})$ to zero leads to the well-known closed-form CV-MMSE solution [18]

$$\mathbf{w}_{\mathrm{CMMSE}} = (\mathbf{P}\mathbf{P}^H + 2\sigma_n^2\mathbf{I}_L)^{-1}\mathbf{p}_1, \tag{9}$$

where $\mathbf{I}_L$ denotes the $L \times L$ identity matrix. An adaptive implementation of the CV-MMSE solution can readily be realised by substituting the stochastic gradient $-(b_1(k) - y(k))^*\mathbf{x}(k)$ for $\nabla J_{\mathrm{MSE}}(\mathbf{w})$ in the steepest-descent gradient algorithm, leading to the following CV-LMS algorithm [18]

$$\mathbf{w}(k+1) = \mathbf{w}(k) + \mu(b_1(k) - y(k))^*\mathbf{x}(k), \tag{10}$$

where μ is the step size.

3.2. Real-valued minimum mean square error design

For BPSK systems, the beamformer's desired output $b_1(k)$ is RV. The CV-MMSE solution minimises the MSE (7), which can be decomposed into the two parts

$$J_{\mathrm{MSE}}(\mathbf{w}) = E[(b_1(k) - y_R(k))^2] + E[y_I^2(k)] = J_{\mathrm{rpMSE}}(\mathbf{w}) + J_{\mathrm{ipMSE}}(\mathbf{w}), \tag{11}$$

where $y_I(k) = \Im[y(k)]$ is the imaginary part of $y(k)$. It is clearly that the CV-MMSE solution attempts to simultaneously minimise the MSE between the desired signal and the real part of the beamformer's output as well as the energy of the imaginary part of the beamformer's output. However, the beamformer's decision depends only on $y_R(k)$. Minimising $J_{\mathrm{ipMSE}}(\mathbf{w})$ does not contribute to improving the beamformer's performance. Rather it imposes an unnecessary constraint on the solution and wastes the antenna array resource.

It is also clear that a more intelligent way of designing the beamformer is to minimise the MSE between the desired output and the real part of the

beamformer's output

$$J_{\text{rpMSE}}(\mathbf{w}) = E[(b_1(k) - y_R(k))^2]. \tag{12}$$

The RV-MMSE solution $\mathbf{w}_{\text{RMMSE}}$ is defined as the weight vector that minimises $J_{\text{rpMSE}}(\mathbf{w})$.[1] Express the received signal vector $\mathbf{x}(k) = \mathbf{x}_R(k) + \mathrm{j}\mathbf{x}_I(k)$ in the RV form

$$\begin{aligned}\mathbf{x}_{\text{e}}(k) &= \begin{bmatrix}\mathbf{x}_R(k)\\ \mathbf{x}_I(k)\end{bmatrix} = \begin{bmatrix}\mathbf{P}_R\\ \mathbf{P}_I\end{bmatrix}\mathbf{b}(k) + \begin{bmatrix}\mathbf{n}_R(k)\\ \mathbf{n}_I(k)\end{bmatrix}\\ &= \mathbf{P}_{\text{e}}\mathbf{b}(k) + \mathbf{n}_{\text{e}}(k),\end{aligned} \tag{13}$$

where $\mathbf{P} = \mathbf{P}_R + \mathrm{j}\mathbf{P}_I$ and $\mathbf{n}(k) = \mathbf{n}_R(k) + \mathrm{j}\mathbf{n}_I(k)$. Note that

$$\begin{aligned}y_R(k) &= \mathbf{w}_R^{\text{T}}\mathbf{x}_R(k) + \mathbf{w}_I^{\text{T}}\mathbf{x}_I(k)\\ &= \begin{bmatrix}\mathbf{w}_R\\ \mathbf{w}_I\end{bmatrix}^{\text{T}}\mathbf{x}_{\text{e}}(k) = \mathbf{w}_{\text{e}}^{\text{T}}\mathbf{x}_{\text{e}}(k).\end{aligned} \tag{14}$$

The gradient of $J_{\text{rpMSE}}(\mathbf{w}_{\text{e}})$ is given by

$$\begin{aligned}\nabla J_{\text{rpMSE}}(\mathbf{w}_{\text{e}}) &= E[-(b_1(k) - y_R(k))\mathbf{x}_{\text{e}}(k)]\\ &= -\mathbf{p}_{\text{e}_1} + (\mathbf{P}_{\text{e}}\mathbf{P}_{\text{e}}^{\text{T}} + \sigma_n^2\mathbf{I}_{2L})\mathbf{w}_{\text{e}},\end{aligned} \tag{15}$$

where $\mathbf{p}_{\text{e}_1}$ is the first column of $\mathbf{P}_{\text{e}}$. Setting the gradient $\nabla J_{\text{rpMSE}}(\mathbf{w}_{\text{e}})$ to zero leads to the closed-form solution

$$\mathbf{w}_{\text{e}_{\text{MMSE}}} = (\mathbf{P}_{\text{e}}\mathbf{P}_{\text{e}}^{\text{T}} + \sigma_n^2\mathbf{I}_{2L})^{-1}\mathbf{p}_{\text{e}_1}. \tag{16}$$

The first L elements of $\mathbf{w}_{\text{e}_{\text{MMSE}}}$ are simply the real part of the RV-MMSE solution $\mathbf{w}_{\text{RMMSE}}$ and the last L elements of $\mathbf{w}_{\text{e}_{\text{MMSE}}}$ form the imaginary part of $\mathbf{w}_{\text{RMMSE}}$.

To derive a sample-by-sample adaptive implementation of the RV-MMSE solution, first note that the gradient of $J_{\text{rpMSE}}(\mathbf{w})$ is

$$\nabla J_{\text{rpMSE}}(\mathbf{w}) = E[-(b_1(k) - y_R(k))\mathbf{x}(k)]. \tag{17}$$

Substituting $\nabla J_{\text{rpMSE}}(\mathbf{w})$ with the stochastic gradient, namely $-(b_1(k) - y_R(k))\mathbf{x}(k)$, leads to the following RV-LMS algorithm:

$$\mathbf{w}(k+1) = \mathbf{w}(k) + \mu(b_1(k) - y_R(k))\mathbf{x}(k). \tag{18}$$

3.3. Minimum bit error rate design

As recognised by Chen et al. [13], the best strategy is to choose $\mathbf{w}$ by directly minimising the system's BER. Following the notations used in [13,20], let us denote the $N_b = 2^M$ number of possible transmitted symbol sequences of $\mathbf{b}(k)$ as $\mathbf{b}^{(q)}$, $1 \leqslant q \leqslant N_b$. Denote furthermore the first element of $\mathbf{b}^{(q)}$, corresponding to the desired symbol $b_1(k)$, as $b_1^{(q)}$. The noise-free part of the beamformer's output $\bar{y}(k)$ assumes values from the signal state set

$$\mathscr{Y} = \{\bar{y}^{(q)} = \mathbf{w}^H\bar{\mathbf{x}}^{(q)} = \mathbf{w}^H\mathbf{P}\mathbf{b}^{(q)},\ 1 \leqslant q \leqslant N_b\}, \tag{19}$$

and $\mathscr{Y}$ can be partitioned into the two subsets conditioned on the value of $b_1(k)$

$$\mathscr{Y}^{(\pm)} = \{\bar{y}^{(q,\pm)} \in \mathscr{Y} : b_1(k) = \pm 1\}. \tag{20}$$

Thus $\bar{y}_R(k)$ can only take the values from the set

$$\mathscr{Y}_R = \{\bar{y}_R^{(q)} = \Re[\bar{y}^{(q)}],\ 1 \leqslant q \leqslant N_b\}, \tag{21}$$

and $\mathscr{Y}_R$ can be divided into the two subsets conditioned on $b_1(k)$

$$\mathscr{Y}_R^{(\pm)} = \{\bar{y}_R^{(q,\pm)} \in \mathscr{Y}_R : b_1(k) = \pm 1\}. \tag{22}$$

The conditional probability density function (PDF) of $y(k)$ given $b_1(k) = +1$ is a Gaussian mixture defined by

$$p(y|+1) = \frac{1}{N_{sb}}\sum_{q=1}^{N_{sb}}\frac{1}{2\pi\sigma_n^2\mathbf{w}^H\mathbf{w}}\,\mathrm{e}^{-(|y-\bar{y}^{(q,+)}|^2)/2\sigma_n^2\mathbf{w}^H\mathbf{w}}, \tag{23}$$

where $\bar{y}^{(q,+)} \in \mathscr{Y}^{(+)}$ and $N_{sb} = N_b/2$ is the size of $\mathscr{Y}^{(+)}$. Thus, the marginal conditional PDF of $y_R(k)$ is

$$p(y_R|+1) = \frac{1}{N_{sb}}\sum_{q=1}^{N_{sb}}\frac{1}{\sqrt{2\pi\sigma_n^2\mathbf{w}^H\mathbf{w}}}\,\mathrm{e}^{-(y_R-\bar{y}_R^{(q,+)})^2/2\sigma_n^2\mathbf{w}^H\mathbf{w}}, \tag{24}$$

where $\bar{y}_R^{(q,+)} \in \mathscr{Y}_R^{(+)}$. The BER of the beamformer for the desired user 1 with the weight vector $\mathbf{w}$ can be shown to be [13,20]

$$P_E(\mathbf{w}) = \frac{1}{N_{sb}}\sum_{q=1}^{N_{sb}} Q(g^{(q,+)}(\mathbf{w})), \tag{25}$$

where

$$Q(u) = \frac{1}{\sqrt{2\pi}}\int_u^\infty \mathrm{e}^{-v^2/2}\,\mathrm{d}v \tag{26}$$

and

$$g^{(q,+)}(\mathbf{w}) = \frac{\operatorname{sgn}(b_1^{(q)})\bar{y}_R^{(q,+)}}{\sigma_n\sqrt{\mathbf{w}^H\mathbf{w}}}. \tag{27}$$

The BER can alternatively be computed based on the other subset $\mathscr{Y}_R^{(-)}$. Note that the BER is invariant to a positive scaling of $\mathbf{w}$.

[1] The closed-form of the RV-MMSE solution was pointed out to us by Reviewer 2.

The MBER solution for the beamformer is then defined as the weight vector that minimises the error probability (25)

$$\mathbf{w}_{\mathrm{MBER}} = \arg\min_{\mathbf{w}} P_E(\mathbf{w}). \tag{28}$$

The gradient of $P_E(\mathbf{w})$ with respect to $\mathbf{w}$ is given by

$$\nabla P_E(\mathbf{w}) = \frac{1}{2N_{sb}\sqrt{2\pi}\sigma_n\sqrt{\mathbf{w}^H\mathbf{w}}} \sum_{q=1}^{N_{sb}} \mathrm{e}^{-(\bar{y}_R^{(q,+)})^2/2\sigma_n^2\mathbf{w}^H\mathbf{w}} \times \mathrm{sgn}(b_1^{(q)}) \left(\frac{\bar{y}_R^{(q,+)}\mathbf{w}}{\mathbf{w}^H\mathbf{w}} - \bar{\mathbf{x}}^{(q,+)} \right), \tag{29}$$

where $\bar{y}_R^{(q,+)} = \Re[\mathbf{w}^H\bar{\mathbf{x}}^{(q,+)}] \in \mathscr{Y}_R^{(+)}$. Given the gradient (29), the optimisation problem (28) can be solved using a gradient-based algorithm [13,20,21]. Following the derivations presented in [13,20], an adaptive implementation of the MBER solution can be realised using the LBER algorithm which takes the form of

$$\mathbf{w}(k+1) = \mathbf{w}(k) + \mu \frac{\mathrm{sgn}(b_1(k))}{2\sqrt{2\pi}\rho_n} \mathrm{e}^{-y_R^2(k)/2\rho_n^2}\mathbf{x}(k), \tag{30}$$

where ρ_n is the kernel width.

3.4. Comparison of three designs

We now compare the three beamformer designs for the BPSK system. The CV-MMSE solution minimises the MSE between $b_1(k)$ and $y(k)$. Therefore, the associated conditional signal subset $\mathscr{Y}^{(+)}$ must have a symmetric distribution with respect to the $\Re[y]$ and $\Im[y]$ axes. This imposes an unnecessary constraint and limits the achievable BER performance, since only the distribution of $\mathscr{Y}_R^{(+)}$ influences the BER performance. By removing the unnecessary constraint on $y_I(k)$, the RV-MMSE solution has more freedom in designing a more favourable distribution of $\mathscr{Y}_R^{(+)}$, leading to an improved BER. The minimum distance between the decision threshold $y_R = 0$ and the subset $\mathscr{Y}_R^{(+)}$ ultimately determines the BER. Minimising $J_{\mathrm{rpMSE}}(\mathbf{w})$ does not guarantees maximising this minimum distance. The MBER solution ensures that this minimum distance is maximised and, therefore, the MBER design generally provides a smaller BER than the

Table 1
Comparison of computational complexity per weight update for the three adaptive BPSK beamformers, where L is the dimension of the weight vector

	Multiplications	Additions	$e^{(\bullet)}$ Evaluation
CV-LMS	$8\times L+2$	$8\times L-1$	–
RV-LMS	$4\times L+1$	$4\times L$	–
LBER	$4\times L+4$	$4\times L-1$	1

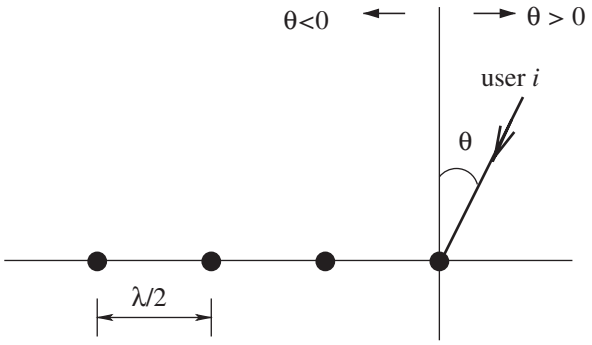

Fig. 1. Geometric structure of the four-element linear array having $\lambda/2$ spacing used in the simulation, where λ is the wavelength.

Table 2
Locations of users in terms of angle of arrival for the simulation

User i	1	2	3	4	5	6	7	8	9	10
AOA θ	0°	10°	−15°	30°	−45°	50°	60°	−55°	−35°	−60°

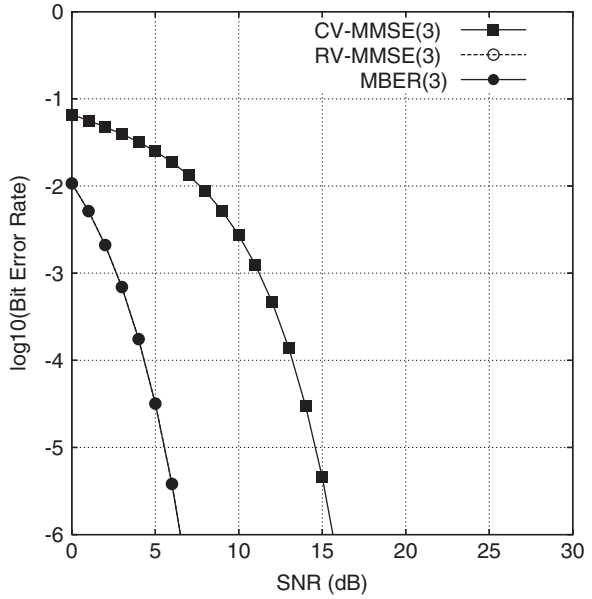

Fig. 2. User-1 BER comparison of three beamforming designs for the four-element array system supporting three users. BERs of the RV-MMSE and MBER beamformers are indistinguishable.

RV-MMSE design, particularly in the so-called overloaded situation.

In order for the CV-MMSE solution to perform adequately, sufficient antenna array resource is required so that the interfering signals can be cancelled. Thus, in order to ensure a correct separation of $\mathscr{Y}_R^{(+)}$ and $\mathscr{Y}_R^{(-)}$ by the decision threshold $y_R = 0$, it is generally required that the number of users is no more than the number of array elements. For the CV-MMSE beamformer, therefore, a system is overloaded if $M > L$. By intelligently concentrating on the real part of the beamformer's output, the RV-MMSE design effectively doubles the degree of freedom in beamforming, since each input $x_l(k)$ is CV or two dimensional. Thus, the RV-MMSE design is capable of supporting users up to twice the number of array elements. Therefore, for the RV-MMSE design, a system is overloaded only if $M > 2L$. The MBER design is not restricted by this limit and is capable of supporting more users. These heuristic discussions will be supported by the simulation results presented in the following section.

Both the CV-MMSE and RV-MMSE designs admit simple closed-form solutions and therefore are computationally attractive. By contrast, the MBER design does not admit a closed-form solution and numerical optimisation must be adopted for obtaining numerical solutions. The RV-LMS algorithm (18) and LBER algorithm (30) are computationally simpler than the CV-LMS algorithm (10). Table 1 compares the computational requirements per weight updating for the three

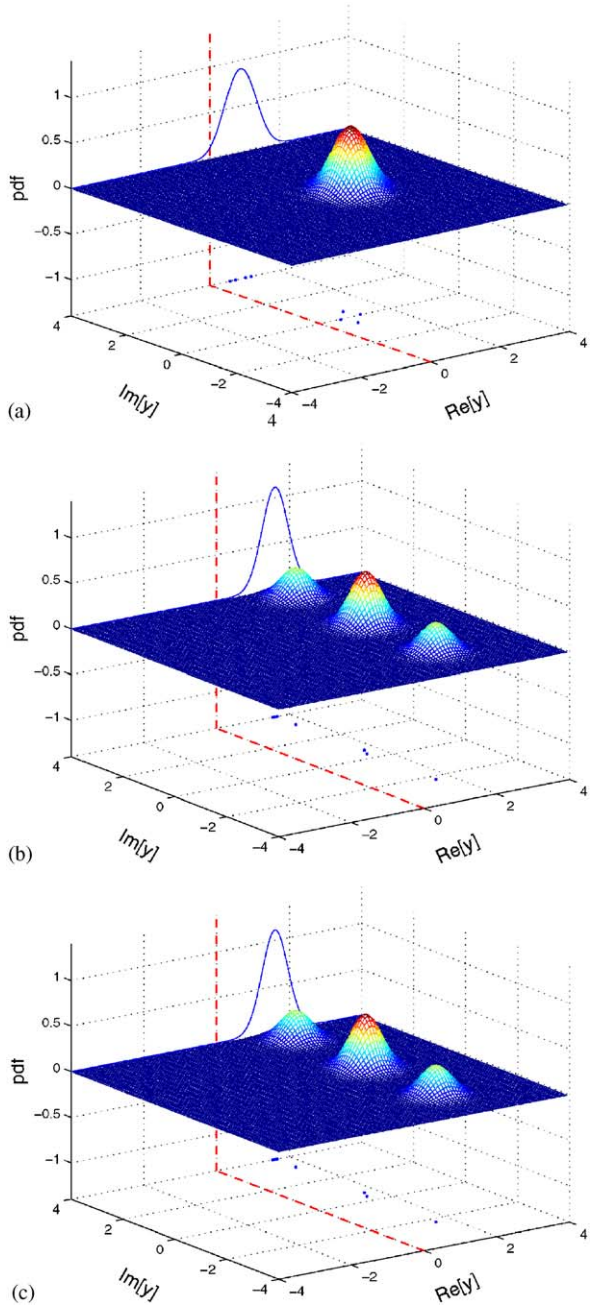

Fig. 3. Conditional probability density functions $p(y|+1)$ (surfaces), marginal conditional probability density functions $p(y_R|+1)$ (curves), signal subsets $\mathscr{Y}^{(+)}$ and $\mathscr{Y}_R^{(+)}$ (points) for the four-element array system supporting three users with SNR = 6 dB: (a) CV-MMSE, (b) RV-MMSE and (c) MBER. The beamformer weight vector is normalised to a unit length.

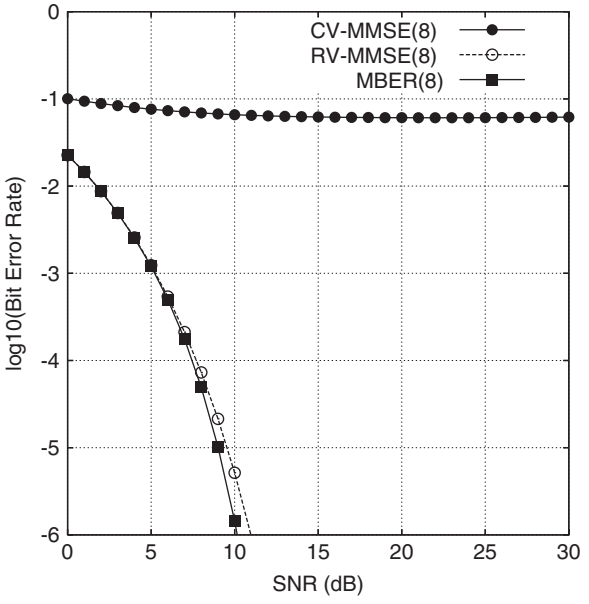

Fig. 4. User-1 BER comparison of three beamforming designs for the four-element array system supporting eight users.

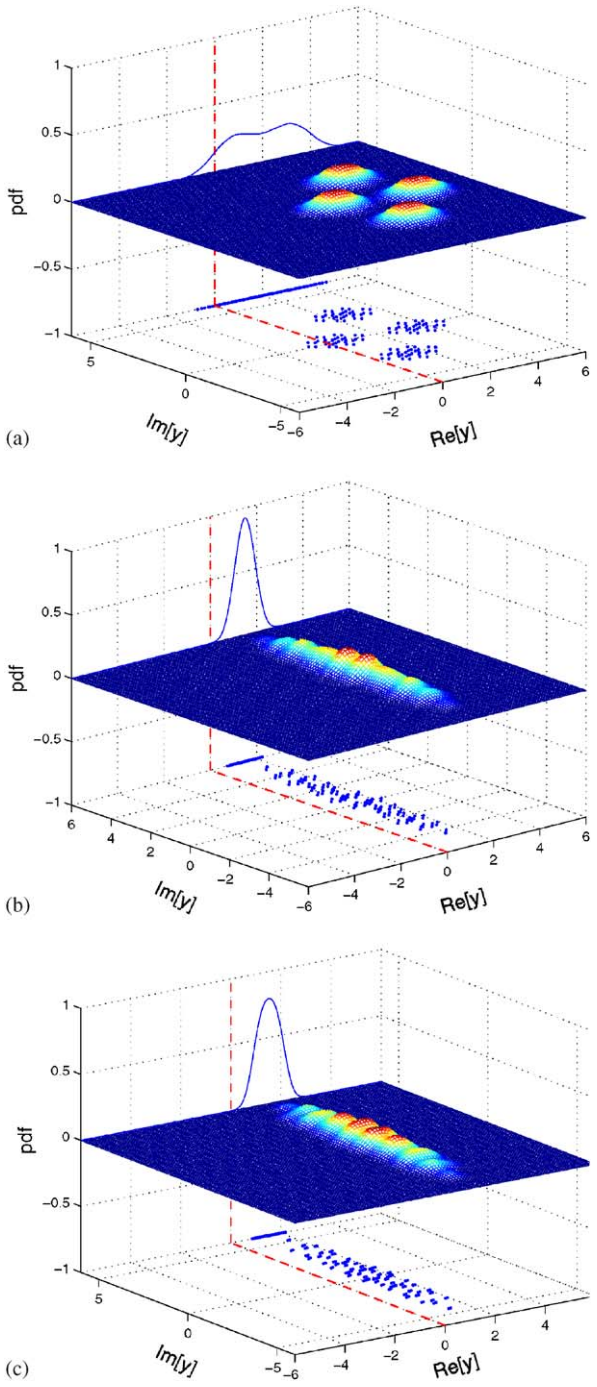

Fig. 5. Conditional probability density functions $p(y|+1)$ (surfaces), marginal conditional probability density functions $p(y_R|+1)$ (curves), signal subsets $\mathscr{Y}^{(+)}$ and $\mathscr{Y}_R^{(+)}$ (points) for the four-element array system supporting eight users with SNR = 8 dB: (a) CV-MMSE, (b) RV-MMSE and (c) MBER. The beamformer weight vector is normalised to a unit length.

adaptive algorithms, where it can be seen that the RV-LMS and LBER algorithms have a similar complexity, which is about half of the complexity required by the CV-LMS algorithm. Convergence analysis for the standard CV-LMS algorithm is well-known [18], which is equally applicable to the RV-LMS algorithm. Convergence analysis of the LBER algorithm is a more difficult task. We point out that the results for the general stochastic gradient-based adaptive algorithm presented in [19] can be applied to the LBER algorithm.

4. Simulation study

The simulated system consisted of a four-element linear antenna array and supported up to $M = 10$ users. Fig. 1 shows the array geometric structure and Table 2 lists the locations of users with respect to the antenna array. The simulated channel conditions were $A_i = 1.0 + \mathrm{j}0.0$ for all users and, therefore, $\mathrm{SIR}_i = 0\,\mathrm{dB}$ for all i. The exact BER of the desired user, user 1, was calculated using formula (25). This includes in the computation of the learning curve for an adaptive algorithm, where at sample k given weight vector $\mathbf{w}(k)$, a point of the learning curve $P_E(\mathbf{w}(k))$ was generated.

Fig. 2 compares the BER performance of the three beamformer designs for the desired user 1 when only the first three users were active. The

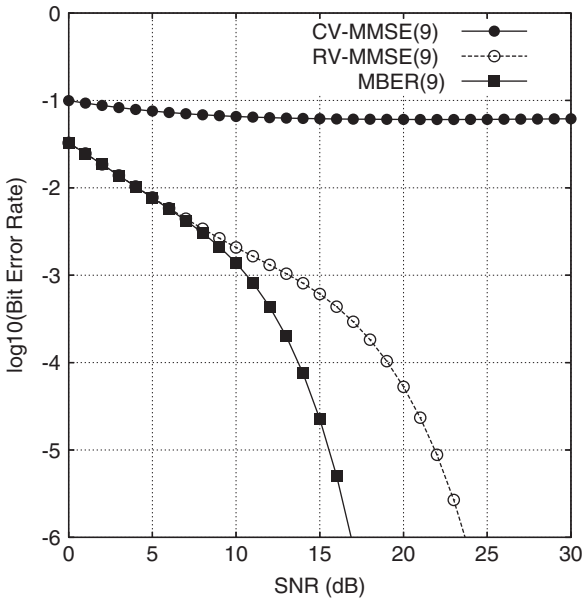

Fig. 6. User-1 BER comparison of three beamforming designs for the four-element array system supporting nine users.

CV-MMSE and RV-MMSE solutions were calculated using formulae (9) and (16), respectively. The MBER solution was obtained numerically using the simplified conjugate gradient optimisation algorithm [13,20,21]. Given SNR = 6 dB, Fig. 3 depicts the conditional PDFs $p(y|+1)$, marginal conditional PDFs $p(y_R|+1)$, signal subsets $\mathscr{Y}^{(+)}$ and $\mathscr{Y}_R^{(+)}$ for the three designs, where the beamformer weight vector $\mathbf{w}$ was normalised to a unit length. It can be seen from Fig. 3(a) that the distribution $p(y|+1)$ was symmetric with respect to the $\Re[y]$ and $\Im[y]$ axes for the CV-MMSE solution. By contrast, the RV-MMSE and MBER designs were not restricted by this symmetric constraint and spread $p(y|+1)$ more widely along the $\Im[y]$ axis, resulting in more favourable marginal distributions of $p(y_R|+1)$ and hence better BER performance than the CV-MMSE design. It can also be seen from Fig. 3(a) that the CV-MMSE solution was able to correctly separate $\mathscr{Y}_R^{(-)}$ and $\mathscr{Y}_R^{(+)}$ and thus provided an adequate BER performance as seen in Fig. 2.

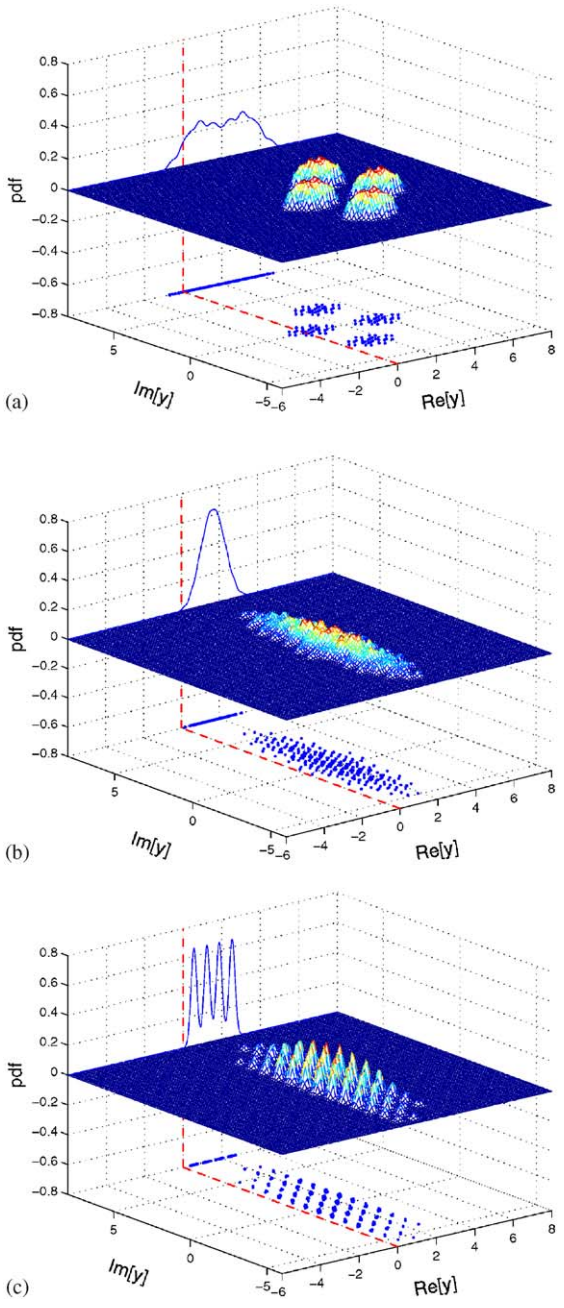

Fig. 7. Conditional probability density functions $p(y|+1)$ (surfaces), marginal conditional probability density functions $p(y_R|+1)$ (curves), signal subsets $\mathscr{Y}^{(+)}$ and $\mathscr{Y}_R^{(+)}$ (points) for the four-element array system supporting nine users with SNR = 15 dB: (a) CV-MMSE, (b) RV-MMSE and (c) MBER. The beamformer weight vector is normalised to a unit length.

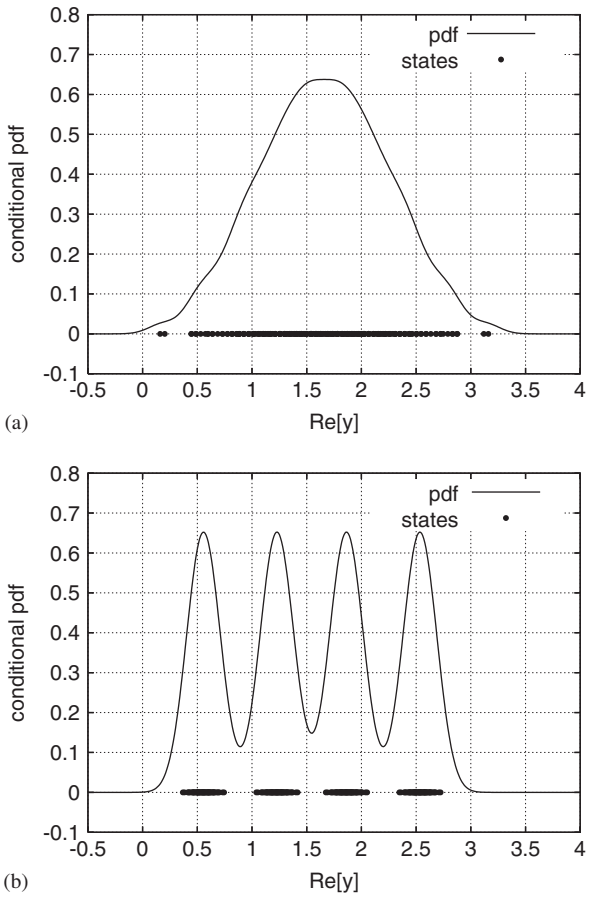

Fig. 8. Marginal conditional probability density functions $p(y_R|+1)$ (curves) and signal subsets $\mathscr{Y}_R^{(+)}$ (points) for the four-element array system supporting nine users with SNR = 15 dB: (a) RV-MMSE and (b) MBER. The beamformer weight vector is normalised to a unit length.

When the number of users was increased to $M > 4$, the CV-MMSE solution was no longer able to provide this desired separation, resulting in a high BER floor. Fig. 4 compares the BER performance of the three beamformer designs when the first eight users were active, while Fig. 5 shows the conditional PDFs $p(y|+1)$, marginal conditional PDFs $p(y_R|+1)$, signal subsets $\mathcal{Y}^{(+)}$ and $\mathcal{Y}_R^{(+)}$ for the three designs, given SNR = 8 dB. It can be seen from Fig. 5(a) that several points of $\mathcal{Y}_R^{(+)}$ were in the wrong side of $y_R = 0$ for the CV-MMSE solution, resulting in the high BER floor as shown in Fig. 4. This system of four receive antennas supporting eight users was heavily overloaded for the CV-MMSE beamformer. By contrast, the system was not overloaded for the RV-MMSE beamformer and the RV-MMSE design was capable of obtaininga distribution that was similar to the MBER design, as can be seen from Fig. 5(b).

Fig. 6 compares the BER performance of the three beamformer designs when the first nine users were active, while Fig. 7 shows the conditional PDFs $p(y|+1)$, marginal conditional PDFs $p(y_R|+1)$, signal subsets $\mathcal{Y}^{(+)}$ and $\mathcal{Y}_R^{(+)}$ for the three designs, given SNR = 15 dB. It can be seen from Fig. 7 that the MBER design attained a more favourable distribution and had a larger minimum distance from the decision threshold $y_R = 0$ to the signal subset $\mathcal{Y}_R^{(+)}$, compared with the RV-MMSE design. In fact the minimum distance for the RV-MMSE solution was 0.16 while this minimum distance was 0.37 for the MBER solution. To see this more clearly, we plot the marginal conditional PDFs $p(y_R|+1)$ and signal subsets $\mathcal{Y}_R^{(+)}$ only in Fig. 8for the RV-MMSE and MBER solutions. The RV-LMS and LBER algorithms were next investigated, and Fig. 9 shows the learning curves $P_E(\mathbf{w}(k))$ of the two adaptive algorithms averaged over 100 runs, given SNR = 15 dB. In Fig. 9(a), training was carried out over the whole length, while in Fig. 9(b), after 40-symbol training, the decision directed (DD) adaptation was invoked by substituting $\hat{b}_1(k)$ for $b_1(k)$.

Fig. 10 compares the BER performance of the three beamformers when all the 10 users were active, while Fig. 11 shows the conditional PDFs $p(y|+1)$, marginal conditional PDFs $p(y_R|+1)$, signal

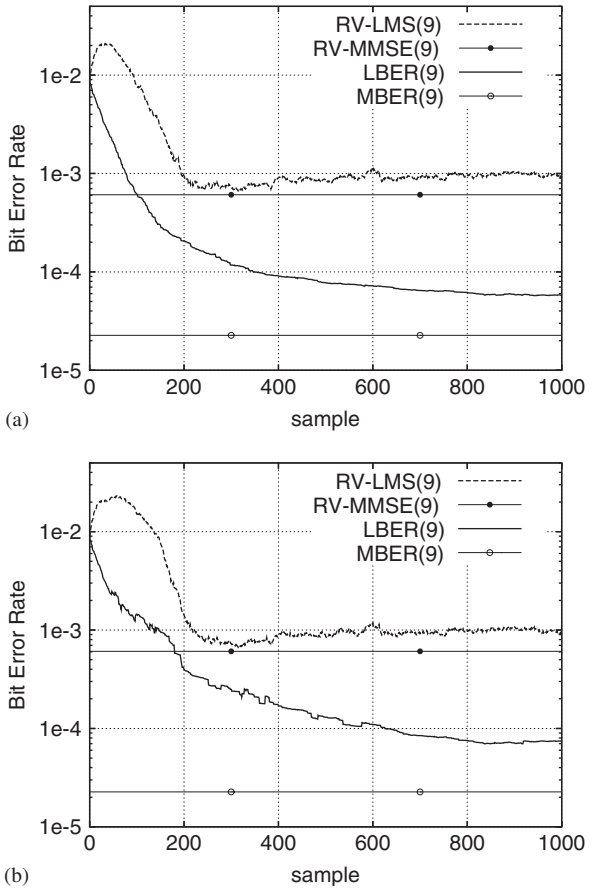

Fig. 9. Learning curves of the adaptive RV-LMS and LBER algorithms averaged over 100 runs for the four-element array system supporting nine users with SNR = 15 dB: (a) training and (b) decision-directed adaptation after 40-symbol training. The step size $\mu = 0.005$ for the RV-LMS, the step size $\mu = 0.01$ and kernel variance $\rho_n^2 = 2\sigma_n^2$ for the LBER.

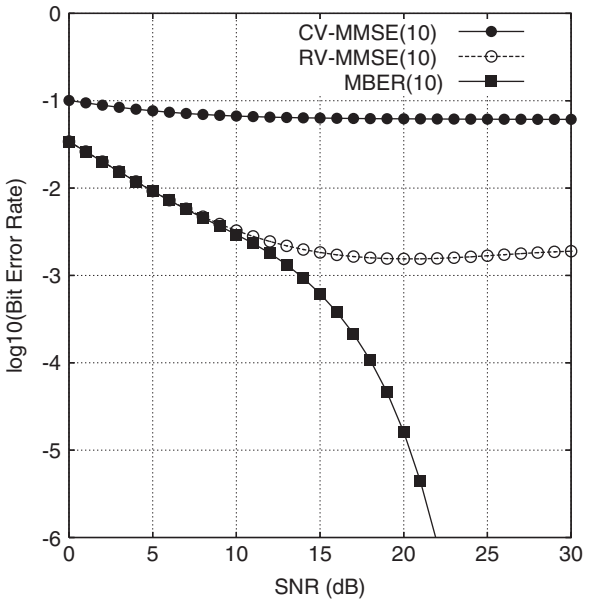

Fig. 10. User-1 BER comparison of three beamforming designs for the four-element array system supporting 10 users.

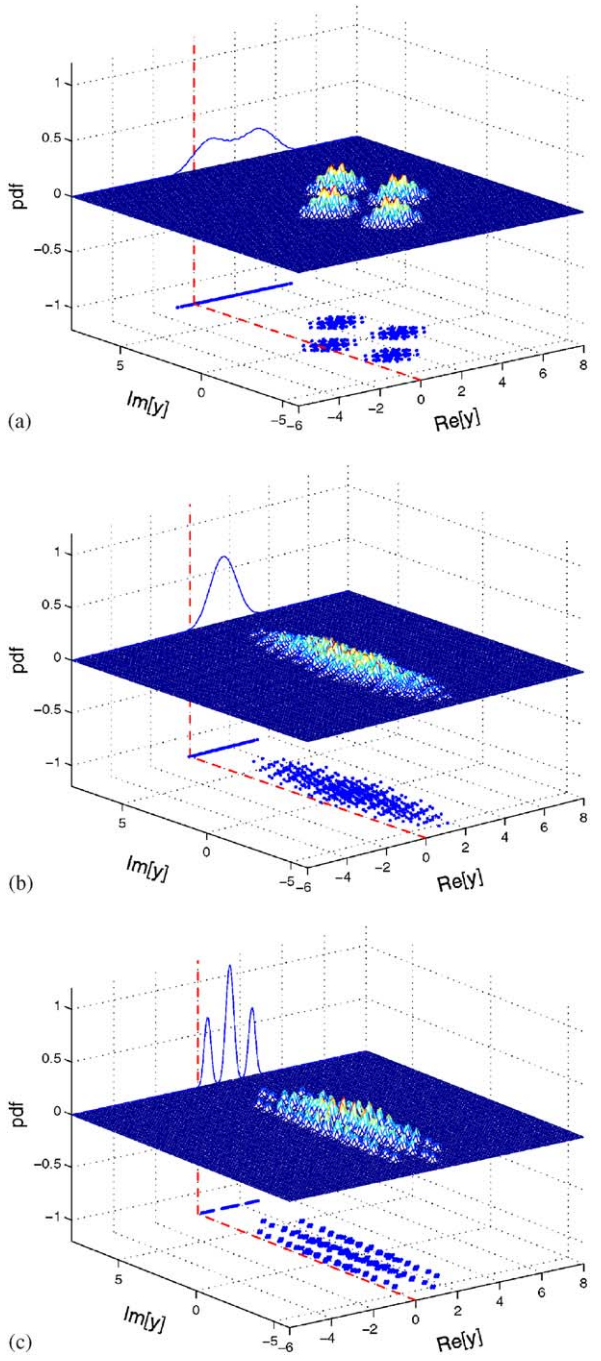

Fig. 11. Conditional probability density functions $p(y|+1)$ (surfaces), marginal conditional probability density functions $p(y_R|+1)$ (curves), signal subsets $\mathcal{Y}^{(+)}$ and $\mathcal{Y}_R^{(+)}$ (points) for the four-element array system supporting 10 users with SNR = 18 dB: (a) CV-MMSE, (b) RV-MMSE and (c) MBER. The beamformer weight vector is normalised to a unit length.

subsets $\mathcal{Y}^{(+)}$ and $\mathcal{Y}_R^{(+)}$ for the three designs, given SNR = 18 dB. Note that in Fig. 11(b) a point of $\mathcal{Y}_R^{(+)}$ is in the wrong side of the decision threshold

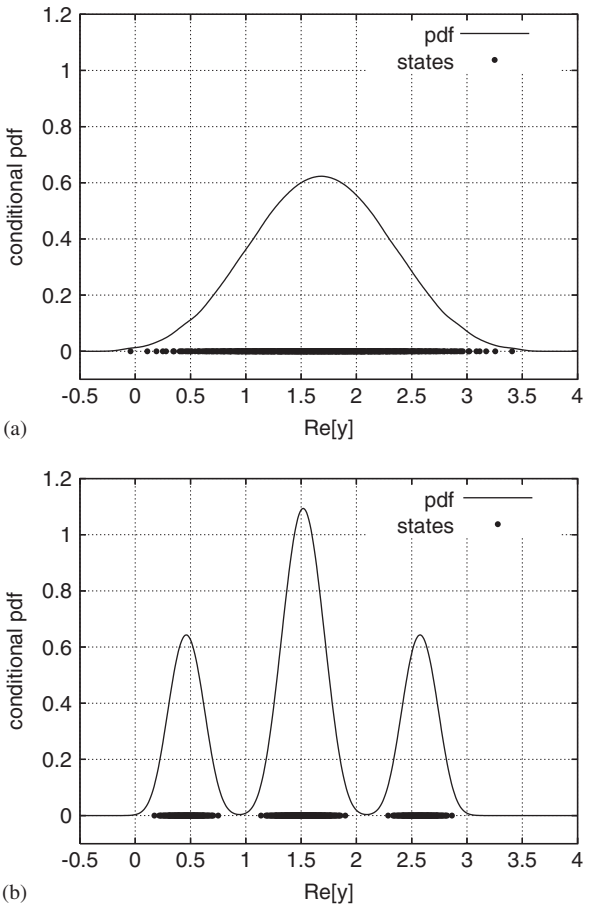

Fig. 12. Marginal conditional probability density functions $p(y_R|+1)$ (curves) and signal subsets $\mathcal{Y}_R^{(+)}$ (points) for the four-element array system supporting 10 users with SNR = 18 dB: (a) RV-MMSE and (b) MBER. The beamformer weight vector is normalised to a unit length.

$y_R = 0$. It is seen that the RV-MMSE solution was no longer capable of separating $\mathcal{Y}_R^{(-)}$ and $\mathcal{Y}_R^{(+)}$ correctly and exhibited a BER floor, since the system was overloaded for the RV-MMSE beamformer. By contrast, the MBER design was still able to separate $\mathcal{Y}_R^{(-)}$ and $\mathcal{Y}_R^{(+)}$ correctlyand provided a much better BER performance than the RV-MMSE design. To see this more clearly, we plot the marginal conditional PDFs $p(y_R|+1)$ and signal subsets $\mathcal{Y}_R^{(+)}$ in Fig. 12 for the RV-MMSE and MBER designs. Finally, the BER performance of the three adaptive beamformers after 100-symbols training are depicted in Fig. 13.

5. Conclusions

An alternative MMSE design has been considered for beamforming-assisted BPSK receiver, which

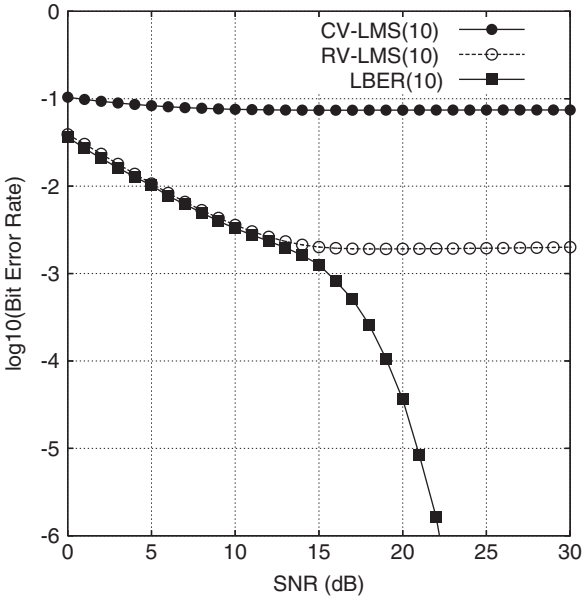

Fig. 13. User-1 BER comparison of three adaptive beamformers for the four-element array system supporting 10 users. Training length is 1000 symbols, the CV-LMS and RV-LMS algorithms have a step size $\mu = 0.002$, while the LBER algorithm has a step size $\mu = 0.01$ and kernel variance $\rho_n^2 = \sigma_n^2$.

minimises the MSE between the real-valued desired output and the real part of the complex-valued beamformer output. This RV-MMSE design offers significant performance enhancement over the standard CV-MMSE design. Moreover, like the CV-MMSE design, the RV-MMSE design admits a simple closed-form solution. It has been demonstrated that the RV-MMSE beamforming solution is capable of obtaining a BER performance that is close to the optimal MBER solution for supporting BPSK users up to twice of the number of antenna array elements. The MBER design is capable of supporting more users than the RV-MMSE design. Adaptive algorithms for implementing these three beamforming designs have also been compared. Both the RV-LMS and LBER-based adaptive beamformers have a similar computational complexity, imposing only half of the computational requirements of the CV-LMS algorithm.

References

[1] J.H. Winters, J. Salz, R.D. Gitlin, The impact of antenna diversity on the capacity of wireless communication systems, IEEE Trans. Commun. 42 (2) (February/March/April 1994) 1740–1751.

[2] J. Litva, T.K.Y. Lo, Digital Beamforming in Wireless Communications, Artech House, London, 1996.

[3] L.C. Godara, Applications of antenna arrays to mobile communications, Part I: Performance improvement, feasibility, and system considerations, Proc. IEEE 85 (7) (1997) 1031–1060.

[4] A.J. Paulraj, C.B. Papadias, Space–time processing for wireless communications, IEEE Signal Process. Mag. 14 (6) (1997) 49–83.

[5] R. Kohno, Spatial and temporal communication theory using adaptive antenna array, IEEE Personal Commun. 5 (1) (1998) 28–35.

[6] P. Petrus, R.B. Ertel, J.H. Reed, Capacity enhancement using adaptive arrays in an AMPS system, IEEE Trans. Veh. Technol. 47 (3) (1998) 717–727.

[7] J.H. Winters, Smart antennas for wireless systems, IEEE Personal Commun. 5 (1) (1998) 23–27.

[8] P. Vandenameele, L. van Der Perre, M. Engels, Space Division Multiple Access for Wireless Local Area Networks, Kluwer Academic Publishers, Boston, 2001.

[9] J.S. Blogh, L. Hanzo, Third Generation Systems and Intelligent Wireless Networking—Smart Antenna and Adaptive Modulation, Wiley, Chichester, 2002.

[10] E.A. Jorswieck, H. Boche, Transmission strategies for the MIMO MAC with MMSE receiver: average MSE optimization and achievable individual MSE region, IEEE Trans. Signal Process. 51 (11) (2003) 2872–2881.

[11] S.A. Mujtaba, MIMO signal processing—the next frontier for capacity enhancement, in: Proceedings of the IEEE 2003 Custom Integrated Circuits Conference, September 21–24, 2003, pp. 263–270.

[12] A. Paulraj, R. Nabar, D. Gore, Introduction to Space–Time Wireless Communications, Cambridge University Press, Cambridge, 2003.

[13] S. Chen, N.N. Ahmad, L. Hanzo, Adaptive minimum bit error rate beamforming, IEEE Trans. Wireless Commun. 4 (2) (2005) 341–348.

[14] S. Chen, L. Hanzo, N.N. Ahmad, A. Wolfgang, Adaptive minimum bit error rate beamforming assisted QPSK receiver, in: Proceedings of the ICC 2004, vol. 6, 2004, pp. 3389–3393.

[15] S. Chen, L. Hanzo, N.N. Ahmad, A. Wolfgang, Adaptive minimum bit error rate beamforming assisted receiver for QPSK wireless communication, Digital Signal Process. 15 (6) (2005) 545–567.

[16] B. Widrow, P.E. Mantey, L.J. Griffiths, B.B. Goode, Adaptive antenna systems, Proc. IEEE 55 (1967) 2143–2159.

[17] L.J. Griffiths, A simple adaptive algorithm for real-time processing in antenna arrays, Proc. IEEE 57 (1969) 1696–1704.

[18] S. Haykin, Adaptive Filter Theory, third ed., Prentice-Hall, Upper Saddle River, NJ, 1996.

[19] R. Sharma, W.A. Sethares, J.A. Bucklew, Asymptotic analysis of stochastic gradient-based adaptive filtering algorithms with general cost functions, IEEE Trans. Signal Process. 44 (9) (1996) 2186–2194.

[20] S. Chen, A.K. Samingan, B. Mulgrew, L. Hanzo, Adaptive minimum-BER linear multiuser detection for DS-CDMA signals in multipath channels, IEEE Trans. Signal Process. 49 (6) (2001) 1240–1247.

[21] M.S. Bazaraa, H.D. Sherali, C.M. Shetty, Nonlinear Programming: Theory and Algorithms, Wiley, New York, 1993.